

Demagnetization Analysis of Ferrite Magnet Using Two-line Approximation Based on Reluctance Network Analysis

D. Momma, Y. Yoshida*, and K. Tajima

Department of Cooperative Major in Life Cycle Design Engineering, Akita Univ., 1-1, Tegata Gakuen-machi, Akita 010-5802, Japan

*Department of Electrical and Electronic Engineering, Akita Univ., 1-1, Tegata Gakuen-machi, Akita 010-5802, Japan

This study presents a method for determining the demagnetization characteristics of ferrite magnets based on reluctance network analysis (RNA). First, an RNA model for determining the operating points of a magnet considering demagnetization using a two-straight-line approximation of the demagnetization curve is discussed. Then, using the proposed model, demagnetization characteristics are determined. Experimental results demonstrate the validity of the proposed method.

Key words: reluctance network analysis, ferrite magnet, demagnetization analysis, two line approximation

1. Introduction

Permanent magnet (PM) motors based on powerful rare-earth magnets are widely used in various applications because of their high-performance characteristics. However, rare-earth magnets may be subject to price rises as the production of such metals is concentrated in a single country. Therefore, the development of highly PM motors without rare-earth magnets is required.

Although the maximum magnetic energy product of ferrite magnets is one tenth that of rare-earth magnets¹⁾, high-efficiency ferrite magnet motors have been reported²⁾. Ferrite magnets in motors are exposed to a large reverse magnetic field to obtain performance equivalent to that of rare-earth magnet motors. Therefore, ferrite magnets are at a risk of demagnetization because of their low coercive force. Thus, it is necessary to consider the demagnetization of ferrite magnets for ferrite magnet motor design.

Reluctance network analysis (RNA) is a useful method to save calculation time in the estimation of the characteristics of PM motors, as reported in previous studies³⁾⁻⁶⁾. However, a demagnetization analysis method using RNA has not yet been proposed.

Because demagnetization analysis using finite element analysis (FEA) has been previously discussed⁷⁾⁻⁸⁾, this method is now applied to RNA. This study presents an RNA model for determining the operating points of ferrite magnets; this model uses a two-line approximation of the demagnetization curve. To verify the accuracy of the proposed model, the calculated results are compared to values obtained from two-dimensional (2D) FEA and experimental results.

2. Derivation of the RNA Model

Fig. 1 shows the shape and specifications of analytical and experimental objects under consideration. Exciting coils are wound around U-shaped cores. Ferrite magnets with a thickness of 2 or 3 mm are sandwiched between the cores. The number of winding turns of exciting coils per leg is 80, and the stack length of the

cores and ferrite magnets is 20 mm.

Fig. 2 illustrates the division of a 2D RNA model. The RNA model is derived in a quarter region of the analysis model shown in the figure, taking advantage of the analytical model's symmetry. In the model, the elements around the air gap are divided with a size of 1.0 mm × 1.0 mm. When the 3-mm-thick magnet is used, the element size of the magnet in the *y*-axis direction is 1.5 mm.

Each divided element is expressed in a 2D-unit magnetic circuit. Fig. 3(a) shows the unit magnetic circuit of the core and air region. In the figure, *l* is the length of the element. The reluctance, R_m , in the unit magnetic circuit is obtained from

$$R_m = \frac{l}{2\mu_s\mu_0(l \times l_s)}, \quad (1)$$

where μ_s is the relative permeability, μ_0 is the permeability of vacuum, and l_s is the stack length of the model. The elements of a ferrite magnet can be expressed as the reluctance and magnetomotive force (MMF), F_m , shown in Fig. 3(b). The reluctance of a ferrite magnet,

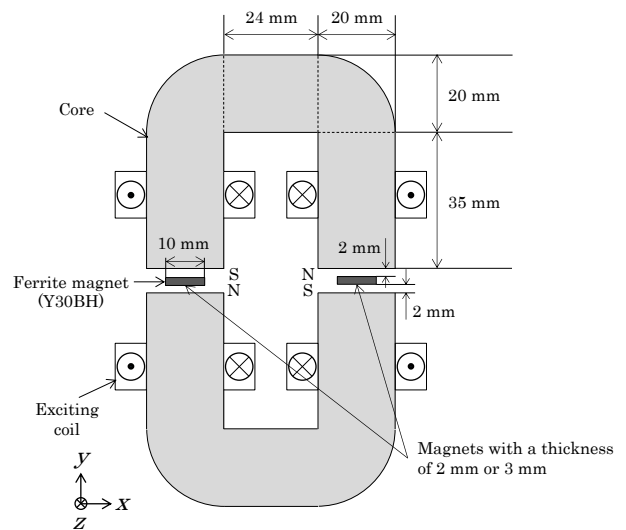


Fig. 1 Specifications of analytical and experimental objects.

R_{mag} , is expressed by

$$R_{mag} = \frac{l}{2\mu_r\mu_0(l \times l_s)}, \quad (2)$$

where μ_r is the magnet's recoil. By connecting all unit magnetic circuits together, the RNA model is obtained.

Fig. 4 illustrates the demagnetization curve of a ferrite magnet, which is approximated by two lines. In the figure, B_r , B_r' , H_c , and H_c' are the residual magnetic flux density before demagnetization, residual magnetic flux density after demagnetization, coercive force before demagnetization, and coercive force after demagnetization, respectively. If there is no demagnetization in a ferrite magnet element, F_m is given by

$$F_m = \frac{B_r l}{2\mu_r\mu_0}. \quad (3)$$

When an operating point of a ferrite magnet is changed by an external magnetic field and becomes less than the knee point, the MMF after demagnetization, F_m' , can be expressed as

$$F_m' = \frac{B_r' l}{2\mu_r\mu_0}. \quad (4)$$

To obtain the residual magnetic flux density after demagnetization (B_r'), $B-H$ and $J-H$ characteristics, where $J = B - \mu_0 H$ as shown in Fig. 5, are used⁹⁾. First, the operating point without considering an external magnetic field, plotted as point a in the figure, is determined by the derived RNA model. The magnetic field at this time is diamagnetic, H_d . At the same time, point b , where a perpendicular line from point a intersects with $J-H$ characteristics, is determined. Then, line l_0 is given as a straight line passing through point b and the origin. Next, the operating point considering an external magnetic field, plotted as point c in the figure, is determined. The external magnetic field, H_{ex} , is calculated as the difference between the magnetic field at point c and H_d . The line, l_0 , is shifted toward the negative direction by H_{ex} without changing the slope to obtain line l_1 . The intersection of $J-H$ characteristics and line l_1 is plotted as point d . When point d is less than the knee point of $J-H$ characteristics, irreversible demagnetization occurs. B_r' is determined as the point where the vertical axis intersects the straight line, which passes through point d and is parallel to $J-H$ characteristics before demagnetization.

3. Demagnetization Analysis of the Ferrite Magnets

Using the proposed RNA model, the demagnetization of the ferrite magnets is determined with an exciting current that produces an external magnetic field opposed to the magnetization direction. Three cycles of a sawtooth wave, shown in Fig. 6, are applied to exciting coils. The maximum value of the current is 4.0 A when the magnet thickness is 2 mm, and 5.5 A when the thickness is 3 mm.

Fig. 7 illustrates the direction of the magnetic flux flowing through the core. This direction is caused by the

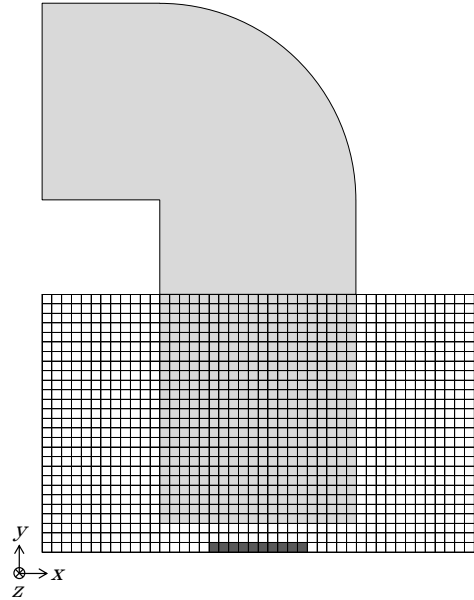


Fig. 2 Division of the RNA model.

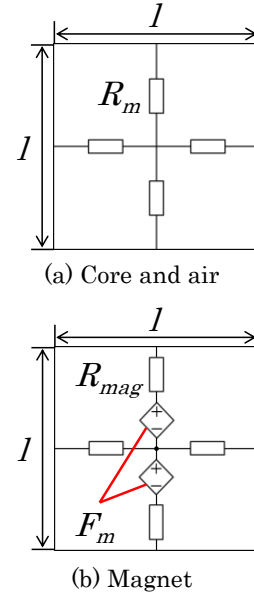


Fig. 3 Unit magnetic circuit.

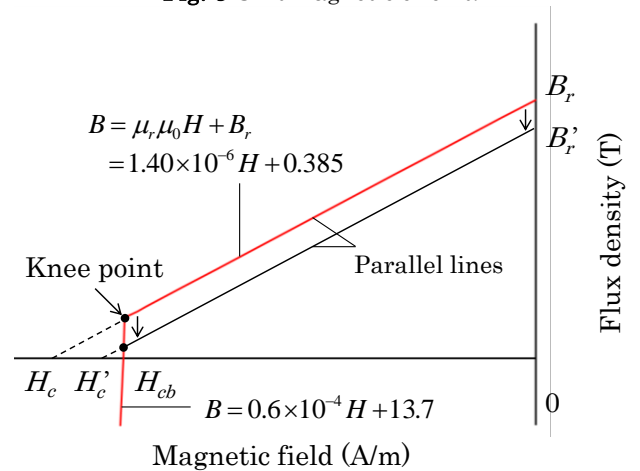


Fig. 4 Demagnetization curve approximated by two lines.

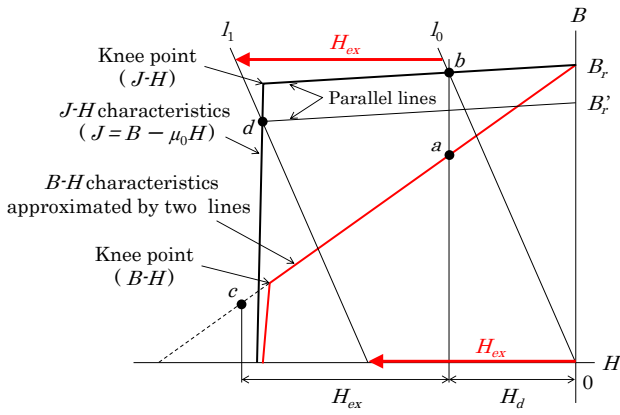


Fig. 5 Calculation method for the residual magnetic flux density after demagnetization.

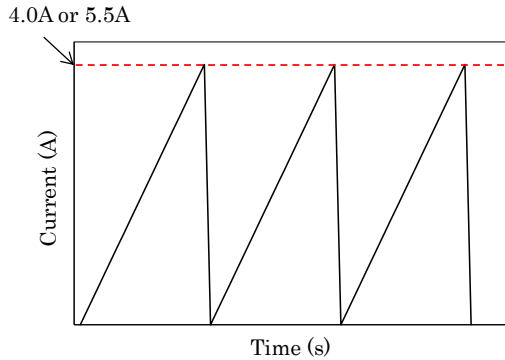


Fig. 6 Waveform of exciting current.

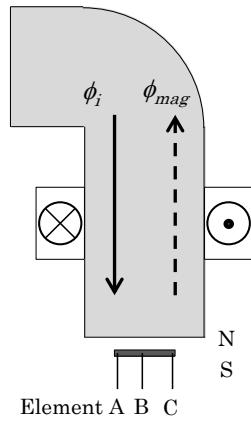


Fig. 7 Direction of magnetic flux and detection points.

winding current and is the inverse of the flux of the ferrite magnet. In the figure, elements A, B, and C are the detection points of demagnetization.

To compare the results from the RNA model with those obtained using FEA, the same calculation as that of RNA was performed using the JMAG-Designer Ver.14.1 software. Fig. 8 shows the mesh distribution of the 2D FEA model. The number of elements of the FEA model is 3,429.

Fig. 9 shows the operating points of element B determined by the RNA and 2D FEA models. It is observed that the data obtained by the proposed RNA model almost agree with the corresponding 2D FEA

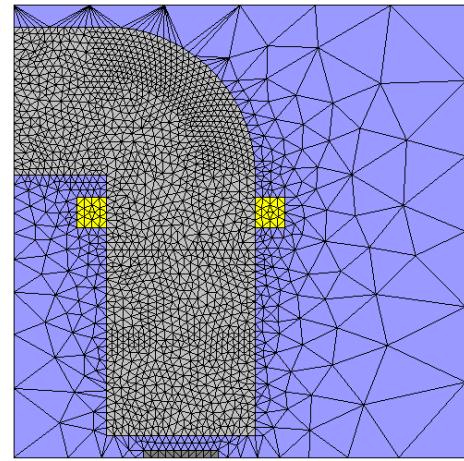
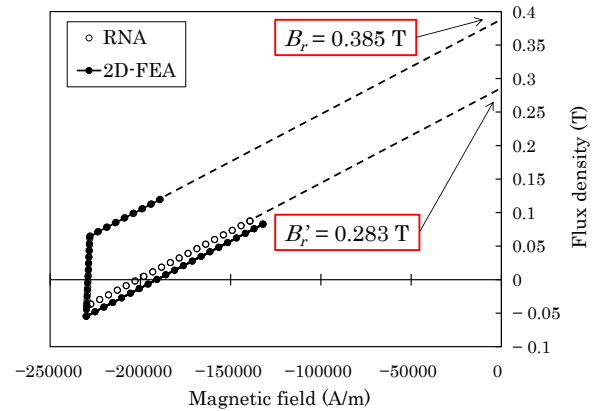
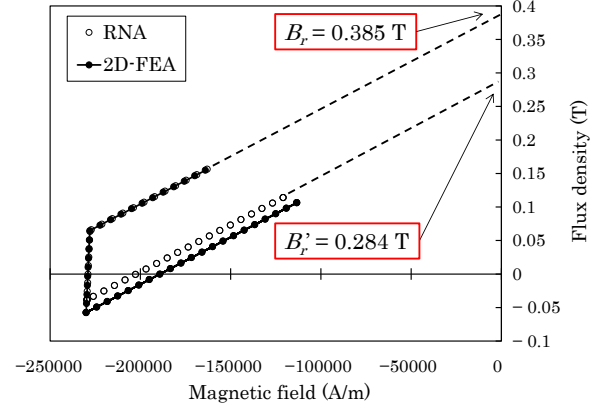


Fig. 8 Mesh distribution of the 2D-FEA model.



(a) Graph for the 2-mm-thick magnet.



(b) Graph for the 3-mm-thick magnet.

Fig. 9 Calculated operating points of element B.

calculation results. The residual flux density of the magnet before demagnetization, B_r is 0.385 T. The calculated residual magnetic flux density after demagnetization by RNA, B_r' is 0.283 T when the magnet thickness is 2 mm, and 0.284 T when it is 3 mm.

Table 1 shows a comparison between the demagnetization factors calculated by RNA and 2D FEA for the 2-mm-thick magnet, and Table 2 shows a comparison of the calculated demagnetization factors by RNA and 2D FEA for the 3-mm-thick magnet. In the tables, the demagnetization factor, D_{fac} , is defined as

Table 1 Demagnetization factors for the 2-mm-thick magnet.

	Element		
	A [%]	B [%]	C [%]
RNA	14.9	26.6	14.9
2D-FEA	14.2	30.4	14.6

Table 2 Demagnetization factors for the 3-mm-thick magnet.

	Element		
	A [%]	B [%]	C [%]
RNA	12.7	26.3	12.7
2D-FEA	7.9	31.0	8.0

Table 3 Interlinkage magnetic flux of ferrite magnets.

	2 mm		3 mm	
	before [Wb]	after [Wb]	before [Wb]	after [Wb]
RNA	0.0236	0.0182	0.0308	0.0239
2D-FEA	0.0236	0.0173	0.0308	0.0229

follows:

$$D_{fac} = \left(1 - \frac{B_r'}{B_r}\right) \times 100. \quad (5)$$

Demagnetization factor at the center of the magnet is greater than that at either end. The calculated values obtained from the proposed model almost agree with those obtained from 2D FEA.

Table 3 shows a comparison of the interlinkage magnetic flux of the ferrite magnets calculated via RNA and 2D FEA. After demagnetization, the interlinkage magnetic flux decreased by approximately 25 % for both magnet thickness.

The number of time steps of the proposed model and 2D FEA model is 64 for three cycles of the sawtooth wave. The calculation times of the proposed and 2D FEA models are 17 s and 58 s, respectively.

4. Comparison with Experimental Results

To verify the calculation accuracy of the RNA model, the calculated values were compared to the measured ones. Fig. 10 shows a photograph of the experimental apparatus; Fig. 10(a) is an exposed view. The supporters are sandwiched between the cores to fix the positions of the cores and magnets. Fig. 10(b) shows an assembled experimental setup. Fig. 11(a) shows the conditions of the experiment, and Fig. 11(b) shows the detection point of the magnetic flux density of the ferrite magnet. The magnetic flux density was determined using a gauss meter (GM-301, Denshijiki Kogyo); the average values of the surface magnetic flux density were obtained from 10 measurements with magnets of the same size.

Fig. 12 shows the comparison of the magnetic flux density of the magnet surface before and after demagnetization. The DC input current is 4.0 A when the magnet thickness is 2 mm and 5.5 A when it is 3

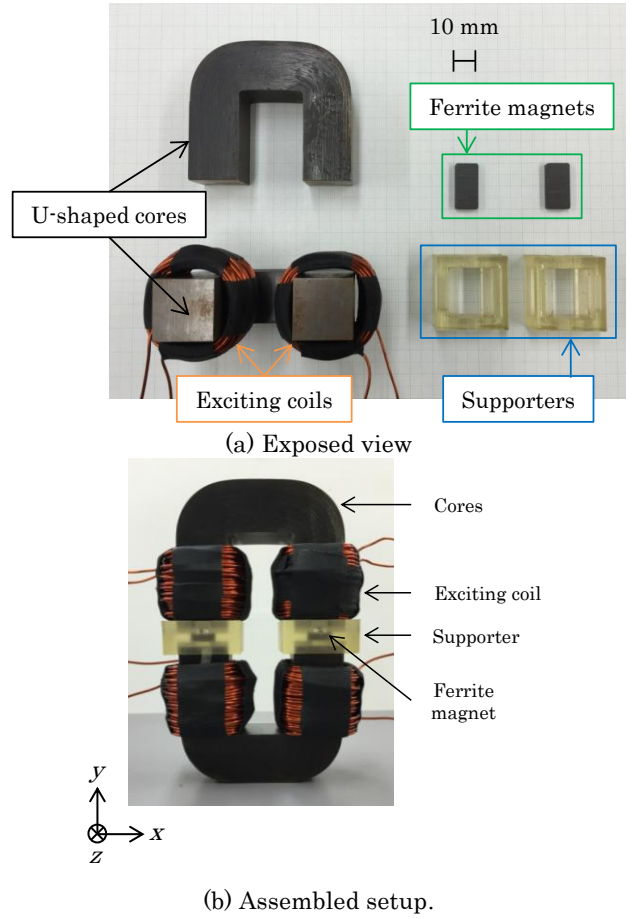


Fig. 10 Photographs of the experimental apparatus.

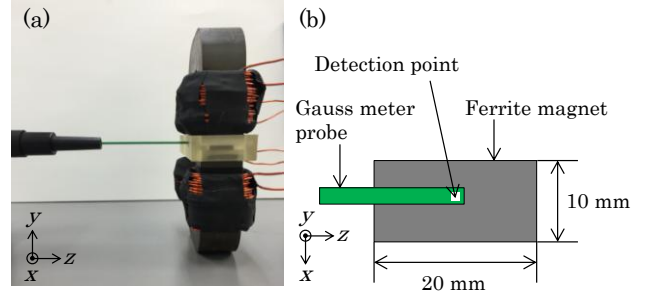
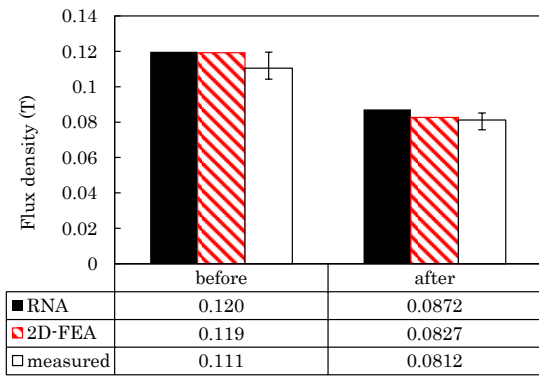


Fig. 11 (a) Measurement setup. (b) Detection point of the magnetic flux density.

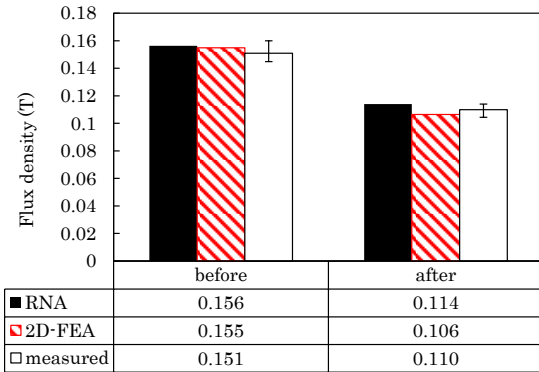
mm. In the figure, the error bars denote the maximum and minimum the measured values. It is concluded that the magnetic flux density determined by the proposed RNA model almost agrees with the corresponding 2D FEA calculated and measured values.

5. Conclusions

This study presented the demagnetization analysis of a ferrite magnet based on RNA. In the proposed model, the demagnetization curve of the magnet was approximated by two lines to estimate the magnetic flux density before and after demagnetization. The validity of the proposed RNA model has been demonstrated by comparing the calculated results with 2D FEA calculation results and experimental results.



(a) Graph for the 2-mm-thick magnet.



(b) Graph for the 3-mm-thick magnet.

Fig. 12 Comparison of magnetic flux densities of magnets.

References

- 1) M. Sagawa, M. Hamano, and M. Hirabayashi: *Eikyujishaku -Zairyokagaku to Oyo-* (in Japanese), p. 16 (Agune Gijutsu Center, Tokyo, 2007).
- 2) M. Sanada, Y. Inoue, and S. Morimoto: *IEEJ Trans. IA*, 13, 12, 1401-1407 (2011).
- 3) K. Nakamura, K. Saito, and O. Ichinokura: *IEEE Trans. Magn.*, 39, 3250-3252 (2003).
- 4) K. Nakamura, M. Ishihara, and O. Ichinokura: *17th International Conference on Electrical Machines (ICEM 2006)*, PSA1-16 (2006).
- 5) K. Nakamura and O. Ichinokura: *13th International Power Electronics and Motion Control Conference (EPE-PEMC 2008)*, 441 (2008).
- 6) Y. Yoshida, K. Nakamura, O. Ichinokura, and K. Tajima: *IEEJ Journal IA*, 3, 6, 422-427 (2014).
- 7) A. Yamagiwa, K. Aota, Y. Sanga, H. Takabayashi and M. Natsumeda: *IEE JAPAN*, RM-03-41 (2003) [in Japanese].
- 8) Y. Osawa and A. Yamagiwa: *IEEJ*, RM-13-62 (2013) [in Japanese].
- 9) <https://www.hitachi-metals.co.jp/products/auto/el/pdf/hg-a2-b.pdf> (As of January 09, 2016) [in Japanese].

Received Oct. 20, 2015; Revised Jan. 10, 2016; Accepted Mar. 21, 2016